LINKÖPING UNIVERSITY

Linköping, Spring term
June 2019
Bachelor thesis 15 hp

Mechanical Behaviour of a Polypyrrole Based Active Guidewire

Ángel López Cuartas anglo342 970427-T155
Andrés García López andga318 971202-T154

Supervisor: Edwin Jager
Laboratory supervisor: Jose Gabriel Martinez Gil
Examiner: Jonas Stålhand

Bachelor thesis for the degree of Mechanical Engineering
LIU-IEI-TEK-G--19/01693—SE

Department of Management and Engineering (IEI)
Department of Physics, Chemistry and Biology (IFM)

Acknowledgements

We would like to thank Dr. Edwin Jager for being our supervisor during this thesis and for his guidance throughout this semester. We thank to Jose Gabriel Martinez Gil for his implication and help during this semester. We also thank to Jonas Stålhand who has been our examiner and for his guidance in the mechanic field. Especially, thanks to everyone for offering us this project.

We would like to thank our home universities for giving us the opportunity of enjoying this experience and being able to develop in other areas.

Last but not least, we would like to thank to our families and friends for giving us support during this year and keep us motivated during the thesis period.

Abstract

The medical field has suffered a great evolution during the last years and it can be reflected in the minimal invasive surgeries' development. These kinds of surgeries are important because have reduced the mishaps during medical interventions using guidewires.

To decrease the risk and to facilitate the surgeries, the implementation of conducting polymers in these guidewires can achieve the necessary bending to drive these tools through the desired path. This is achieved by attaching a conducting polymer, called Polypyrrole (PPy), in one side of the guidewire tip, and applying small voltages (<1V) getting the desired bending decreasing the medical intervention time.

In this project, it has been developed a theoretical model to predict the bending of these kinds of tools knowing the force of the PPy can do. In order to obtain it, experiments varying the dimensions of these polymers have been carried out in an electrolyte solution called NaDBS with 2 types of guidewires ("ZIPwire Hydrophilic Guidewire" and "Amplatz SuperStiff guidewire" of Boston Scientific). These results are compared with the results previously obtained checking how they fit with the reality.

INDEX

1. Introduction 1
   1.1. PolyPyrrole 2
   1.2. Electrolytes 3
   1.3. Electropolymerization of PPy 3
   1.4. Guidewires 3
   1.5. Thesis Purpose 4
2. Materials 4
   2.1. Guidewires 4
      2.1.1. ZIPwire™Hydrophilic Guide Wire (Boston Scientific) 4
      2.1.2. Amplatz Super Stiff™Guidewire (Boston Scientific) 5
   2.2. Sodium dodecylbenzenesulfonate (NaDBS) 5
   2.3. Polypyrrole 5
   2.4. Potentiostat (PalmSens) 5
   2.5. Counter electrode 6
   2.6. Working electrode 6
   2.7. Reference electrode 6
   2.8. Electrolyte Cell 7
   2.9. Series 300B dual mode servo system (Cambridge Technology) 7
   2.10. Camera 7
   2.11. Clamp stand 7
   2.12. Micrometre 7
3. Methods 8
   3.1. Beam Theory 8
   3.2. Set Up 8
   3.3. Deflection measurement (Matlab) 9
   3.4. Apply of Potential (EmSens) 9
   3.5. Force Measurement 9
   3.6. “EI” coil value (Ansys) 10
4. Modelling Procedure 10
   4.1. First Approximation 11
   4.2. Final Catheter Model 13
   4.3. Force Transformation 16
   4.4. Gravity effect 18

5. Experimental and Theoretical Results & Discussion 20
5.1. ZIPwire™ Hydrophilic Experience 20
5.1.1. Stiffness ∑EI 20
5.1.2. Measurements and Calculus Comparison 22
5.1.2.1 Experimental Deflection Measurement 22
5.1.2.2 Constant Length, Different Thicknesses 22
5.1.2.3 Constant Thickness, Different Lengths 24
5.1.2.4 Final Results: 26
5.1.3. Polypyrrole "EI" Effect 29
5.1.4. Numerical Gravity Effect 29
5.2. Amplatz Super Stiff™ Experience 30
5.2.1. Stiffness ∑EI 30
5.2.2. Measurements and Calculus Comparison 31
6. Conclusion and Future work 34
References 35

List of figures

Figure 1: Guidewire structure 4
Figure 2: Potentiostat 6
Figure 3: Reference Ag/AgCl electrode 6
Figure 4: Electronic micrometre 7
Figure 5: Left: Setup Right: Setup Scheme 8
Figure 6: Force measurement setup 9
Figure 7: Real PPy force and acting force on the beam 10
Figure 8: Torque along the wire 11
Figure 9: Left: Deflection. Right: Curvature angle 13
Figure 10: Zoom in the inner part of the longitudinal section of the ZIPwire 13
Figure 11: Zoom in the longitudinal section of the Amplatz wire 14
Figure 12: Tip force scheme 16
Figure 13: Gravity force approximation 18
Figure 14: Gravity force scheme 19
Figure 15: ZIPwire 20
Figure 16: Wire approximation and cross-section area 21
Figure 17: Bending of the sample 22
Figure 18: Stabilization 23
Figure 19: 2.5C length 9 cm comparison 23
Figure 20: 5C length 9cm comparison 24
Figure 21: Experimental 7.5C Length 9cm Deflection vs position 24
Figure 22: 7.5C length 2cm comparison 25
Figure 23: 7.5C length 4cm comparison 25
Figure 24: 7.5C length 6cm comparison 26
Figure 25: PPy thickness vs charge 26
Figure 26: Volumetric force vs potential 27
Figure 27: Experimental Deflection vs Thickness considering 7.5 C 28
Figure 28: Experimental Deflection vs Thickness 28
Figure 29: Experimental Deflection vs PPy length 29
Figure 30: Coil structure 30
Figure 31: Amplatz coil tip ANSYS 31
Figure 32: PPy attachment scheme 32
Figure 33: Amplatz: 2.5C Deflection 32
Figure 34: Amplatz: 5C Deflection 33

List of tables

Table 1: ZIPwire Manufacturing dimensions 5
Table 2: Amplatz Manufacturing dimensions 5
Table 3: ZIPwire measured dimensions 20
Table 4: Obtained forces transformation 1 27
Table 5: Obtained forces transformation 2 27
Table 6: Experimental and theoretical final tip deflections and angles comparison 28
Table 7: PPy stiffness effect 29
Table 8: Gravity influence 29
Table 9: Amplatz coil measurements 30
Table 10: Ansys Amplatz tip displacement 31
Table 11: Amplatz coil measurements 32
Table 12: Theoretical displacement for a known PPy thickness 32

1. Introduction

In the last decade, due to the development of video cameras and image, the methods of surgery have suffered changes with the use of catheters and guidewires in order to reduce damage and to have an easier access where, if a conventional surgery were made, there would be high possibilities to have problems (1). This way of surgery is being used in many areas in the medicine such as intravascular ultrasound, treatment of thromboembolic diseases, heart problems, etc, which means that they can be used in many body systems. This way of Minimally Invasive Surgeries has solved those problems and furthermore have many advantages e.g. reduction of pain, faster recuperation post-surgery or low risk of infection (2).

Nowadays active controllable catheters and guidewires are not being widely used, and they are controlled in the body vessels by pulling and torqueing through them, this causes a great dependence on the skills of the doctor to know exactly the procedure not to have mishaps, and this dependence cause damage in the body system because of the complicated body anatomy. To deal with this, there have been arising technologies to control the orientation and deflection of the tip of the catheter to decrease complications (3).

The apparition of the conducting polymers (CPs), and the properties when applying a charge such as the variation in volume, colour change or charge storage, has shown the wide range of uses and their usefulness resulting in the application of them in many different areas. The property that most concerns us is the deformation response of the CP in front of an electrical signal and the use of them as artificial muscles (4). This has raised in the possibility to use them for the bending of the catheter tip and how to incorporate it. More concretely, there have been emerging investigations of one specific conducting polymer which is the PolyPyrrole (PPy) showing the interesting response (force generates or time to increase volume) when applying a potential and how to take advantage of it to control the bending of the guidewire tip and improve medical techniques.

For the attachment of the conducting polymer in the catheter, the PolyPyrrole will be used as polymer actuator only in one side of the tip as was researched by Krogh and Jager, and the direction of it can be controlled by rotating the guide wire (5). As it has been stated, the good electromechanical response of the PolyPyrrole with charge is a great advantage to control the catheter tip. Moreover it has another properties such us it is biocompatible not to cause additional problems, and it is due to the great response to low voltages (<2 V) not to cause problems in the organism (3).

This work will be focused in the use of this technology in the urinary system since the potential applied is low enough. It will be carried out from a mechanical engineering view of point to elaborate a model in which the deflection could be measured for a specific potential, and how the research object depends on different boundary characteristics. In short, the investigation will have a great dependence on the Beam Theory and boundary conditions to have feasible results and elaborate the appropriate conclusions.

First, we need to establish and give a more focused explanation of the characteristics of the components such as the PolyPyrrole or engineering theory and in this way, have an overview of the necessary research knowledge.

1.1. PolyPyrrole

In order to carry out these surgeries, a polymer called PolyPyrrole (PPy) is used. Some of its properties are his muscle-like actuation behaviour (its potential as an electrochemically driven artificial muscle) and its use as electromechanical sensor. Moreover, there are some facts to consider, like the cycle life, mechanical stability or slow response (6).

In this thesis it has been focused in the medical field, (e.g. medical implants, human assist devices, minimally invasive surgical). For the purpose of the polymer in this field, it is going to actuate as an electrochemically driven artificial muscle, and not as an electromechanical sensor. Conductive polymers which works as artificial muscles can be divided into two groups:

The first one, the electronic electroactive polymers, that have some properties such as large strains and high work densities, but also there are some disadvantages, like that the actuation stresses are low, or the main one which is that it requires of high voltages (>1kV) and it could create safety concerns in the human body.

The second group are the ionic electroactive polymers, in where an electrolyte phase (usually liquid) is required for the movement of the ions and requires low actuations voltages (<10V). In this group, we can subdivide the actuator between ionic polymer metal composites (IPMC) and the conducting polymers. In the second group, conducting polymers, the one who is going to be studied is the PolyPyrrole, which has been found to be one of the most effective artificial muscle actuator due to its electrochemical stability, low cost, and biocompatibility (6).

Polypyrrole (PPy) is a type of organic polymer formed by the polymerization of pyrrole. It is a solid with the formula $H(C_4H_2NH)_nH$. In this work, PPy will be fabricated on the surface of different types of ureteral guidewires. The elastic moduli of PPy is >0.2 GPa and can reach up to 7 GPa (7).

The most important properties of the PPy are the good conducting response in both fields, electrical and thermal. Also, it has good mechanical properties (8).

The behaviour of the Conducting Polymers, specifically the PPy doped with macroions can be expressed in the following equation:

$$\underset{\text{Neutral chains}}{\left[\left(pPy^{0}\right)\left(MA^{-}\right)_{n}\left(C^{+}\right)_{n}\right]_{s}} \xleftrightarrow{Red/Oxid} \underset{\text{Oxidized chains}}{\left[\left(pPy^{n+}\right)\left(MA^{-}\right)_{n}\right]_{s}} + n\left(C^{+}\right)_{sol} + n\left(e^{-}\right)_{metal} \qquad \text{eq. (a)}$$

In this equation (4), which is a redox process (from the left to the right it is an oxidation process, and from the right to the left it is a reduction process), 's' means solid, 'sol' is solution, PPy is the PolyPyrrole chains, 'C^{+}' represent a cation and 'MA^{-}' are the macroions trapped in the solid during polymerization. This process is called 'p-doping' since the reactions produce positive charges on the polymeric chains.

With these macroions, the polymer shrinks during oxidation and swells during reduction, instead of swells during oxidation and shrinks during reduction if the material did not have macroions (4).

1.2. Electrolytes

An electrolyte is a solution (generally liquid) in which there are free ions which means that it behaves like an electric conductor. The importance of the electrolytes is that muscles and neurons in the human body are activated by biologic electrolytes, which work with low electric currents (9).

For this project, NaDBS will be used, which is a really extended electrolyte used in the medical field and investigations.

1.3. Electropolymerization of PPy

Electropolymerization is the process to synthetize the PPy.

The PolyPyrrole films are prepared in an electrochemical cell from an aqueous solution of NaDBS and Pyrrole. In this solution there are a working electrode, two large electrodes used as counter electrodes in order to obtain an electric field and an Ag electrode used as reference electrode. With all these electrodes, a constant anodic current density is applied during a specific time (4). During this process, the DBS^- macroions are trapped into the solid solution.

In order to electropolymerize the polymer material, it is necessary that the side of the catheter in which the PPy is going to be, is bare. Once this is done, the attachment of the polymer material takes place during electropolymerization. The time periods depend on the thickness of the PPy film, and they can be from 30 minutes to 12 hours.

1.4. Guidewires

With the emergence of the guidewires 30 years ago and the continuous evolution of them until now, there have been a great change in the medical procedures meaning that nowadays those mechanisms are a very extended way of intervention causing the less mishaps during it (10).

To understand the importance and the confidence on those technologies, should be stated the characteristics which make this a safe and an extended medical technique.

The components of the guide wire and its structure is the initial point to understand why of its use and how it works.

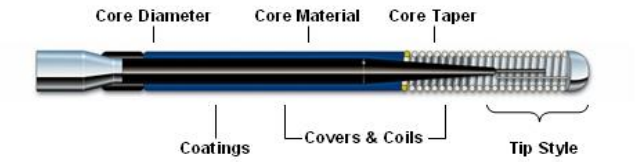

Figure 1: Guidewire structure

As it can be seen in Figure 1 (11), there is not a complicated and complex tool which is formed basically by the coatings, the cores and the coil.

As it has been stated previously one of the benefits is the less pain, and here has an important influence the coatings since it must be soft and smooth to benefit the sliding through tortuous vessels. This characteristic is accomplished by the coating, where the most extended one is the use of a hydrophilic coating. The function of the core is the stiffness since it needs to be enough stiff to the movements such as pulling and torqueing, and to facilitate the navigation (12). Two types are the most common, the nitinol core, which is an alloy of titanium and nickel; or a steel core. The material of the core classifies the guidewires for different medical fields depending on the steerability and trackability (13). Talking about the tip, the most extended design is composed by a cylindrical coil on the tip which makes easier the bending and consequently the navigation.

1.5. Thesis Purpose

The aim of this project is to study how a PPy based active guidewire deflects and how the variation of the PPy dimensions affects to the bending. This study is carried out developing a theoretical model to predict this bending.

2. Materials

2.1. Guidewires

The dimensions of the guidewires (radius along the core due to its tapered shape) have been measured with a micrometre that will be explained later.

2.1.1. ZIPwire™Hydrophilic Guide Wire (Boston Scientific)

ZIPwire is used to study the movement and force of the Polypyrrole and have an overview of its behaviour. The guidewire is formed by a Nitinol (NiTi) core wire, a Shape Memory Alloy metal which can retain a deformation in a temperature and then recover its original shape; a polyurethane jacket and a hydrophilic coating (PTFE). The metal core contributes to the torque and the stiffness to have a good control of the catheter and deal with obstructions and tortuous anatomies. And the coating has the purpose to low the friction and makes the intervention softer. Moreover, the tip of this wire has a lower diameter, facilitating the deformation and in consequence, the navigation throw the vessels (14).

Total Diameter (in)	Total Diameter (mm)	Length (cm)	Tip style
0.035	0.889	150	Straight

Table 1: ZIPwire Manufacturing dimensions

It has been used 6 ZIPwire Hydrophilic, 3 with different PPy coating lengths, 2cm, 4cm and 6cm respectively and 3 different thicknesses (2,5C, 5C and 7,5C). The unit of measurement to talk about thickness will be Coulombs, because the thicknesses of the PPy studied are too small and in this way is easier. The relation between thickness and charge (C) is stated in Figure 25.

2.1.2. Amplatz Super Stiff™Guidewire (Boston Scientific)

The main characteristic of this guidewire is its floppy tip which simplifies the navigation and generates a greater displacement when the PPy acts. The core diameter is made by stainless steel 316 and it decreasing to the tip; it has a flat-wire floppy coil which is found throughout the catheter contributing to the torque motion. It is covered with a non-conductive PTFE coating softening throw its way. This combination of core and coil provides an extra strength and stability (15).

Diameter (in)	Diameter (mm)	Length (cm)	Tip style	Tip length (cm)
0.038	0.9652	145	Straight	6

Table 2: Amplatz Manufacturing dimensions

2.2. Sodium dodecylbenzenesulfonate (NaDBS)

In order to charge the polymer and shrink or swell it NaDBS has been used. The electrolyte concentration is 0.1M NaDBS in water making that the Na+ cations come into the polymer in reduction and go out into the oxidation (16).

2.3. Polypyrrole

As stated above, PPy used has macroions od DBS trapped into the polymer, so it shrinks when oxidation, and swells when reduction. It is attached to only one side of the guidewire.

It is electropolymerized at 0.7 V during the necessary time to reach the desired charge in a aqueous solution 0.1 M NaDBS, and 0.1 M Py at room temperature.

2.4. Potentiostat (PalmSens)

In order to get a determined potential, it is used a potentiostat. It controls the potential to the working electrode, which will be explained detailed after.

The model is “EmStat” of PalmSens which has eight current ranges from 1 nA to 100 mA, 2 mm banana connectors for Working, Counter, Reference, Sense (EmStat+) and Ground (17).

The system works by maintaining the potential of the working electrode at a constant level with respect to the reference electrode, making the current ionizes the polymer. Thus, the polymer swells or shrinks in function of the potential applied (negative or positive potential respectively).

Figure 2: Potentiostat

2.5. Counter electrode

The counter electrode (also called auxiliary electrode) is used to transfer the input potential with respect to the reference electrode to the working electrode. The purpose of these electrodes is to complete the circuit and to let the charge to flow. Consequently, these electrodes are made from inert material, e.g. carbon, platinum, gold or stainless steel, and they must be bigger than the working electrode in order to ensure that there is no current limitation (18). In this case, the counter electrode is a steel mesh.

2.6. Working electrode

The working electrode is the one which is studied. It usually has a favourable redox behaviour. The working electrode are the samples in which the polymer is attached, and the polymer absorbs ions or reject from the solution.

2.7. Reference electrode

In order to make the experiment, a reference electrode is needed. It has a fixed electrochemical potential and it is used to apply a potential difference to the electrode. There is no current along it (19). This electrode is a glass-bodied electrode, and use a porous junction made from a ceramic material. The material of it is Ag/AgCl from Basi (20).

Figure 3: Reference Ag/AgCl electrode

2.8. Electrolyte Cell

It is the recipient where it is the electrolyte. It must be big enough in order to put all the electrodes inside and the Redox reaction can occur. The measures of the cell are 12x10x3 cm. In order to measure the displacement of different parts of the catheter, a graph paper has been stuck behind the cell.

2.9. Series 300B dual mode servo system (Cambridge Technology)

The Series 300B is a system which measures mechanical responses of muscles such as the force keeping the displacement constant of displacement keeping constant force. The force that acts in the tip of the catheter when is applied the same charge that is used for the displacement will be measured by a level. It returns voltage signal, so from the stress it transforms it into a voltage. This system measures the force perpendicular to the longitudinal axis of the guidewire.

In order to obtain this force through the potential, this equation is used:

$$F = \frac{V}{0{,}2}\, g, \qquad \text{where g is the gravity } (9{,}8\ {}^{m}/_{s^2})$$

2.10. Camera

The camera used is the rear camera of 13-megapixel (f/1.9) of the Samsung Galaxy J6.

2.11. Clamp stand

In order to get the same than it is obtained in the theoretical model, the catheter is clamped in the upper part with two arms, to ensure that the boundary conditions are met to get a cantilever beam.

2.12. Micrometre

Measurements of the catheter have been done with an electronic micrometre with tolerance ± 0.001 mm from Mitutoyo, as it can see in the following picture:

Figure 4: Electronic micrometre

3. Methods

3.1. Beam Theory

Euler–Bernoulli beam theory is the method used to obtain the deflection and the angle for all the points of the wire. The procedure starts integrating the equation below to obtain deflection of the beam which is subjected to lateral forces. It is supposed that the beam is static equilibrium, so you can get the final state.

$$M = -EI\frac{d^2w}{dx^2}$$

The catheter can be treated as a cantilever beam, where the PPy generates a distributed axial force which can be transformed into a distributed moment along the layer of this polymer, as it will be explained and developed lately.

3.2. Set Up

The setup is composed by the cell, cables, clamps, and the electrodes (working, reference and counter) as is shown in the following figure:

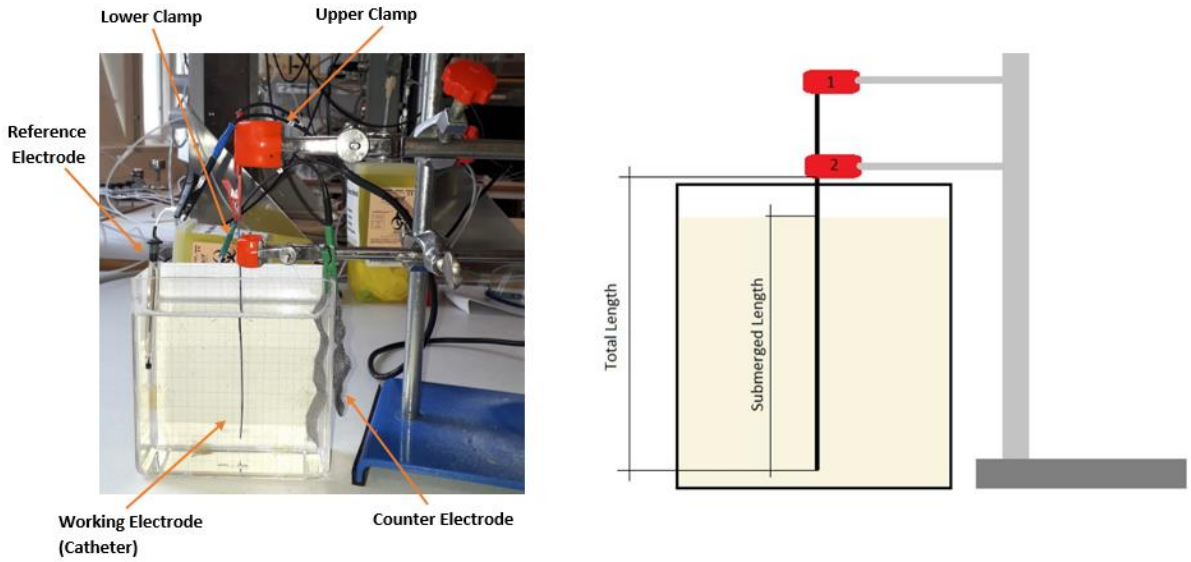

Figure 5: Left: Setup Right: Setup Scheme

In order to establish the boundary conditions such as zero movement or angle at the position x=0 if it is measured from the root to the tip, two clamps should be used to hold the sample in a fixed position. In the Figure 5 the upper clamp is needed to hold the crocodile that connects the sample to the potentiostat and obtain the necessary data. The lower clamp is needed to have zero deflection and angle in that position, so this is the starting point (x=0) from which the measurements are going to be done.

3.3. Deflection measurement (Matlab)

The displacement is measured with the use of Matlab with the function `imtool`. The displacements are calculated by relating pixels distances from the initial position (before potential) to the end position (after potential). The real distances are measured taken as reference the number of pixels of one square (1 mm).

3.4. Apply of Potential (EmSens)

For the application of potential, the electrodes which are in contact with the electrolyte are connected to the potentiostat by a 2 mm banana connector from the counter, working and reference electrodes to the potentiostat. Therefore, the EmSens is connected to the computer. The program which runs the potential application and reads the current from the sample is the PSTrace which is given with the EmStat.

As the potential difference between the PPy used and the reference electrode is around -0.3V, the values applied in the program (PSTrace) for the experimental measurements have been -1V for the reduction (swelling) and +0.5V for the oxidation (shrinking), meaning a potential difference of around ± 0.7 with respect to the PPy. And then -0.7V and +0.2V respectively meaning a potential difference around ± 0.4.

3.5. Force Measurement

In order to measure the forces done by the PolyPyrrole when it shrinks and swells, a device called Series 300B dual mode servo system is used. The potential data from the displacement measurements is introduced as an input in a program called Nova 2.1. The tip of the sample is in contact with the Series 300B sensor. With the movement of the sample the point force at the tip is given.

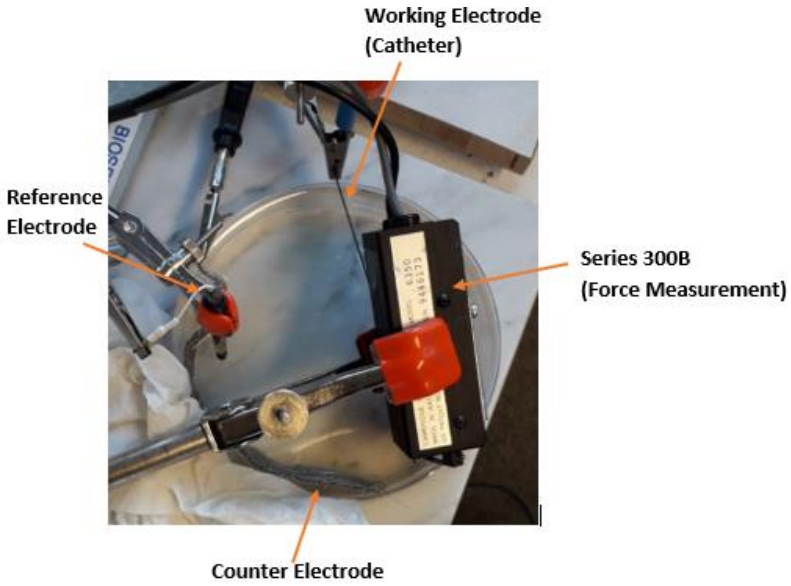

Figure 6: Force measurement setup

3.6. "EI" coil value (Ansys)

In the Amplatz SuperStiff guidewire, the value of the second moment of area "I" is difficult to be calculated because it has a coil. Instead, the "EI" product of is going to be calculated.

The procedure of how the EI is calculated will be explained more in depth later.

4. Modelling Procedure

As stated previously, the Euler Bernoulli Beam Theory governs the behaviour of a beam, which depends on necessary boundary conditions to study the real behaviour of the body subject to a force.

The catheter can be considered as a cantilever beam as shown in the Figure 7:

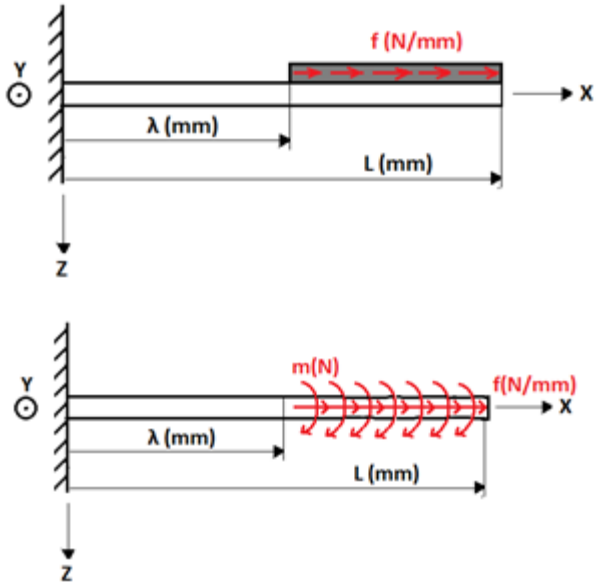

Figure 7: Real PPy force and acting force on the beam

In this figure, the grey zone of the upper scheme is the PPy attached to the beam. Due to its swelling at the reduction, it produces a longitudinal distributed force.

To study the movement, the force from the upper scheme is transformed into a longitudinal force "f" applied in the middle of the beam in the x direction and a distributed torque "m" as shown in the fFigure 7:

About the boundary conditions, the position x=0 contributes to stablish the structure. At this position the deflection and the angle of curvature of the beam subject at a known force are zero ($w(0) = w'(0) = 0$).

As said in the Beam Theory, the torque produced along the beam is the only external force that affects to the deflection. This torque reaction along the x direction is represented in Figure 8:

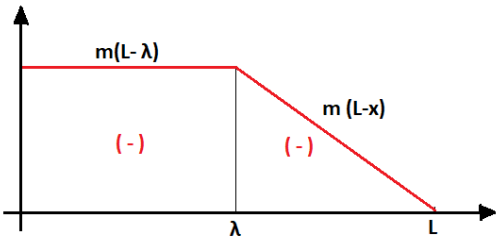

Figure 8: Torque along the wire

Values of x within the range $0 \leq x \leq \lambda$:

$$M = -m(L - \lambda) \quad (1)$$

Values of x within the range of $\lambda \leq x \leq L$

$$M = -m(L - x) \quad (2)$$

4.1. First Approximation

In the first approximation the deflection and angle of curvature are going to be studied without considering the elimination of the coating jacket from lambda to x=L to attach PPy.

From Euler-Bernoulli we know: $M = -\sum(EI)w'' \quad (3)$

For $0 \leq x \leq \lambda$

By inserting Eq. (1) into eq. (3) and integrating two times over "x" it is obtained:

$$m(L - \lambda) = \sum(EI)w''$$

$$m(L - \lambda)x + C_1^L = \sum(EI)w' \quad (4)$$

$$m(L - \lambda)\frac{x^2}{2} + C_1^L x + C_2^L = \sum(EI)w \quad (5)$$

To get the values of the constants C_1^L and C_2^L, the boundary conditions must be applied at x=0. At this point as it has been stated previously, it is known that the deflection (w) and the angle of curvature (w') are zero (w=0; w'=0):

$$C_1^L = C_2^L = 0$$

Once these values are known the equations for the range $0 \leq x \leq \lambda$ are:

- $w(x) = \frac{m(L-\lambda)}{2\sum(EI)}x^2 \quad (6)$
- $w'(x) = \frac{m(L-\lambda)}{\sum(EI)}x \quad (7)$

For $\lambda \leq x \leq L$

By inserting Eq. (2) into Eq. (3) and integrating two times over "x" it is obtained:

$$m(L - \mathrm{x}) = \sum(\mathrm{EI})w''$$

$$m\left(Lx - \frac{x^2}{2}\right) + C_1^R = \sum(\mathrm{EI})w' \ (8)$$

$$m\left(L\frac{x^2}{2} - \frac{x^3}{6}\right) + C_1^R\mathrm{x} + C_2^R = \sum(\mathrm{EI})w \ (9)$$

To obtain the constants C_1^R and C_2^R, a continuity between the the point inmediatly to the left (x= $-\lambda$) of x= λ of the point inmediatly to the right left (x= $+\lambda$). Thus, w(-λ) = w($+\lambda$) and w'(-λ) = w'($+\lambda$) should be accomplished.

To obtain C_1^R, w'(-λ) = w'($+\lambda$) is applied with the eqs. (7) and (8):

$$m\left(L\lambda - \frac{\lambda^2}{2}\right) + C_1^R = M(L - \lambda)\lambda \ \rightarrow$$

$$\rightarrow \ C_1^R = \mathrm{m}\left(\mathrm{L}\lambda - \lambda^2 - \mathrm{L}\lambda + \frac{\lambda^2}{2}\right) \rightarrow$$

$$\rightarrow \ C_1^R = -\frac{1}{2}\mathrm{m}\lambda^2 \ (10)$$

Equalling eqs. (6) and (9) (w(-λ) = w($+\lambda$)) and inserting eq. (10), $\mathrm{C_2^R}$ is obtained:

$$m\left(L\frac{\lambda^2}{2} - \frac{\lambda^3}{6}\right) - \frac{1}{2}\mathrm{m}\lambda^3 + C_2^R = \frac{1}{2}\mathrm{m}(\mathrm{L} - \lambda)\lambda^2 \ \rightarrow$$

$$\rightarrow m\frac{1}{2}\left(L - \frac{\lambda}{3}\right)\lambda^2 - \frac{1}{2}\mathrm{m}\lambda^3 + C_2^R = \frac{1}{2}\mathrm{m}(\mathrm{L} - \lambda)\lambda^2 \ \rightarrow$$

$$\rightarrow C_2^R = \frac{1}{6}\mathrm{m}\lambda^3 \ (11)$$

Once these values are known the equations for the range $\lambda \leq x \leq$ L are:

- $w(x) = \frac{m}{6\sum(\mathrm{EI})}(-x^3 + 3Lx^2 - 3\lambda^2 x + \lambda^3)$ (12)
- $w'(x) = \frac{m}{2\sum(\mathrm{EI})}(-x^2 + 2Lx - \lambda^2)$ (13)

The $\sum$(EI) of these equations is obtained by:

Imetal(core) $= \frac{\pi r_0^4}{4}$ $\quad r_0 = \frac{d_0}{2}$ $\quad$ Icoating $= \frac{\pi}{4}(r^4 - r_0^4)$ $\quad r = \frac{d}{2}$

$$\sum(\mathrm{EI}) = Emetal * Imetal + \ Ecoating * Icoating$$

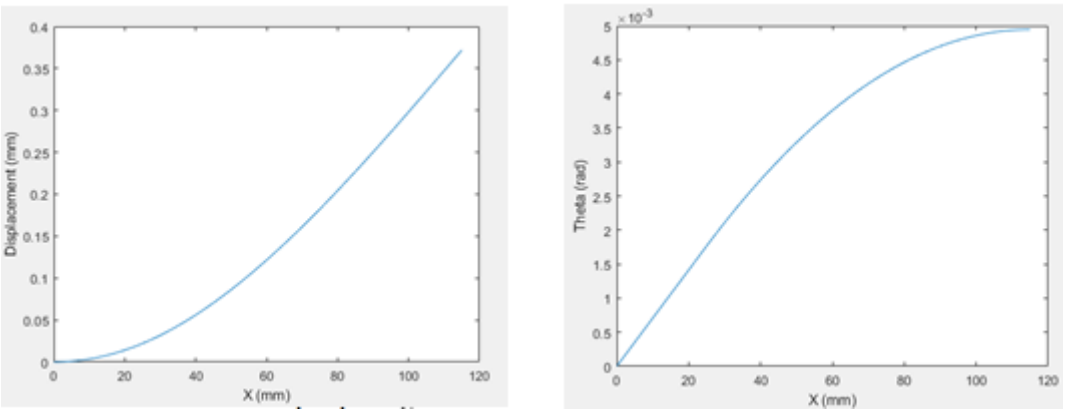

Figure 9: Left: Deflection. Right: Curvature angle

In Figure 9 the tendency of the first approximation eqs. (6), (7), (12) and (13) is correctly fitting the beam theory and the behaviour of a cantilever beam.

The data inserted is arbitrary in order to see if the tendency is accurate to the expected:

Distributed moment (m) = 2E-04 N
Catheter Length =115 mm
PPy length = 90 mm
Metal Core Radius = 0.1588 mm
Metal Core Young's Modulus = 28E+03 N/mm2
Coating Radius = 0.889 mm
Coating Young's Modulus = 500 N/mm2

4.2. Final Catheter Model

Once the simplest model has fitted, is needed to approach to the reality considering a change in the ∑(EI). This change is shown in Figure 10 and Figure 11.

For the attachment of the PPy in the ZIPWire (simplest sample), a piece of the polymer coating should be eliminated creating a different second moment of area "I" along the catheter.

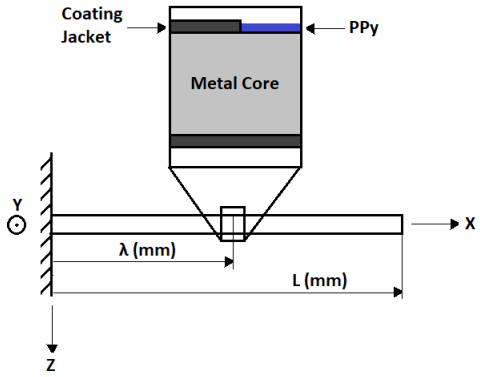

Figure 10: Zoom in the inner part of the longitudinal section of the ZIPwire

About the Amplatz Guidewire (coil tip sample), along the tip there is a floppy coil that contributes to the easy manoeuvring during a medical procedure. This coil has different second moment of area "I" when a force is applied because the deflection is greater on this part.

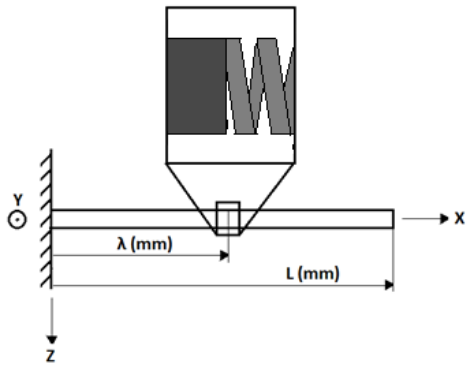

Figure 11: Zoom in the longitudinal section of the Amplatz wire

These stated facts make a more complex model needed. To achieve this purpose, the stiffness along the wire is differentiated at the immediate left and right point of x= λ.

For $0 \leq x \leq \lambda$:

Starting from the equations (1), (2) and (3):

$$0 \leq x \leq \lambda$$

$$m(L-\lambda) = \sum(\mathrm{EI})^{L} w''$$

$$m(L-\lambda)\mathrm{x} + C_1^L = \sum(\mathrm{EI})^{L} \mathrm{w}' (14)$$

$$m(L-\lambda)\frac{x^2}{2} + C_1^L \mathrm{x} + C_2^L = \sum(\mathrm{EI})^{L} w \ (15)$$

For a range of $0 \leq x \leq \lambda$ the Eqs. (16) and (17) are obtained:

- $w(x) = \frac{m(L-\lambda)}{2\sum(\mathrm{EI})^{L}} x^2 \ (16)$
- $w'(x) = \frac{m(L-\lambda)}{\sum(\mathrm{EI})^{L}} x \ (17)$

For $\lambda \leq x \leq L$:

By inserting Eq. (2) into Eq. (3) and integrating two times over "x" it is obtained:

$$m(L-\mathrm{x}) = \sum(\mathrm{EI})^{R} \, w''$$

$$m\left(Lx - \frac{x^2}{2}\right) + C_1^R = \sum(\mathrm{EI})^{R} w' \ (18)$$

$$m\left(L\frac{x^2}{2} - \frac{x^3}{6}\right) + C_1^R \mathrm{x} + C_2^R = \sum(\mathrm{EI})^{R} w \ (19)$$

To obtain the constants C_1^R and C_2^R, the continuity must be applied as before. Thus, w(-λ) = w(+λ) and w'(-λ) = w'(+λ) should be accomplished. When substituting the equations into these equivalences, the equation that corresponds to the range $0 \leq x \leq \lambda$ should use $\sum(\mathrm{EI})^L$ corresponding to the part with coating jacket and the equation for the range $\lambda \leq x \leq L$ should use $\sum(\mathrm{EI})^R$ corresponding to the part with PPy and without coating in the upper side. The $\sum(\mathrm{EI})^L$ and $\sum(\mathrm{EI})^R$ are constants.

To obtain C_1^R, w'(-λ) = w'(+λ) is applied with the eqs. (17) and (18):

$$\frac{\sum(\mathrm{EI})^R}{\sum(\mathrm{EI})^L} m(L-\lambda)\lambda = m\left(L\lambda - \frac{\lambda^2}{2}\right) + C_1^R \rightarrow$$

$$\rightarrow C_1^R = \frac{\sum(\mathrm{EI})^R}{\sum(\mathrm{EI})^L} m(L\lambda - \lambda^2) - m\left(L\lambda - \frac{\lambda^2}{2}\right) \rightarrow$$

$$\rightarrow C_1^R = \mathrm{mL}\lambda\left(\frac{\sum(\mathrm{EI})^R}{\sum(\mathrm{EI})^L} - 1\right) - m\lambda^2\left(\frac{\sum(\mathrm{EI})^R}{\sum(\mathrm{EI})^L} - \frac{1}{2}\right) \quad (20)$$

Equalling eqs. (16) and (19) (w(-λ) = w(+λ)):

$$\frac{\sum(\mathrm{EI})^R}{2\sum(\mathrm{EI})^L} m(L-\lambda)\lambda^2 = m\left(L\frac{\lambda^2}{2} - \frac{\lambda^3}{6}\right) + C_1^R\lambda + C_2^R \rightarrow$$

$$C_2^R = \frac{\sum(\mathrm{EI})^R}{2\sum(\mathrm{EI})^L} m(L-\lambda)\lambda^2 - m\left(L\frac{\lambda^2}{2} - \frac{\lambda^3}{6}\right) - C_1^R\lambda \rightarrow$$

$$\rightarrow C_2^R = \frac{mL\lambda^2}{2}\left(\frac{\sum(\mathrm{EI})^R}{\sum(\mathrm{EI})^L} - 1\right) - \frac{m\lambda^3}{2}\left(\frac{\sum(\mathrm{EI})^R}{\sum(\mathrm{EI})^L} - \frac{1}{3}\right) - C_1^R\lambda \rightarrow$$

Inserting eq. (20):

$$\rightarrow C_2^R = \frac{mL\lambda^2}{2}\left(\frac{\sum(\mathrm{EI})^R}{\sum(\mathrm{EI})^L} - 1\right) - \frac{m\lambda^3}{2}\left(\frac{\sum(\mathrm{EI})^R}{\sum(\mathrm{EI})^L} - \frac{1}{3}\right) - \mathrm{mL}\lambda^2\left(\frac{\sum(\mathrm{EI})^R}{\sum(\mathrm{EI})^L} - 1\right) + m\lambda^3\left(\frac{\sum(\mathrm{EI})^R}{\sum(\mathrm{EI})^L} - \frac{1}{2}\right)$$

$$\rightarrow$$

$$\rightarrow C_2^R = -\frac{mL\lambda^2}{2}\left(\frac{\sum(\mathrm{EI})^R}{\sum(\mathrm{EI})^L} - 1\right) + \frac{m\lambda^3}{2}\left(\frac{\sum(\mathrm{EI})^R}{\sum(\mathrm{EI})^L} - \frac{2}{3}\right) \quad (21)$$

We get these equations inserting (20) and (21) into (18) and (19) for $\lambda \leq x \leq$ L:

$$w(x) = \frac{m}{\sum(\mathrm{EI})^R}\left(\left(L\frac{x^2}{2} - \frac{x^3}{6}\right) + \left(\mathrm{L}\lambda\left(\frac{\sum(\mathrm{EI})^R}{\sum(\mathrm{EI})^L} - 1\right) - \lambda^2\left(\frac{\sum(\mathrm{EI})^R}{\sum(\mathrm{EI})^L} - \frac{1}{2}\right)\right)\mathrm{x} - \frac{L\lambda^2}{2}\left(\frac{\sum(\mathrm{EI})^R}{\sum(\mathrm{EI})^L} - 1\right) + \frac{\lambda^3}{2}\left(\frac{\sum(\mathrm{EI})^R}{\sum(\mathrm{EI})^L} - \frac{2}{3}\right)\right) \quad (22)$$

$$w'(x) = \frac{m}{\sum(\mathrm{EI})^R}\left(\left(Lx - \frac{x^2}{2}\right) + \mathrm{L}\lambda\left(\frac{\sum(\mathrm{EI})^R}{\sum(\mathrm{EI})^L} - 1\right) - \lambda^2\left(\frac{\sum(\mathrm{EI})^R}{\sum(\mathrm{EI})^L} - \frac{1}{2}\right)\right) \quad (23)$$

The eqs. (22) and (23) are more exact than (12) and (13) since it considers the differentiation at the λ point. If $\sum(\mathrm{EI})^R$ and $\sum(\mathrm{EI})^L$ have a close value $\frac{\sum(\mathrm{EI})^R}{\sum(\mathrm{EI})^L} \approx 1$ the equations turn into the eqs. (12) and (13) since many terms get null.

4.3. Force Transformation

In order to measure the real effort of the PPy, which causes the deflection of the catheter, the blocking force at the tip in order to avoid the movement is measured with the "Series 300B dual mode servo system" (the force is shown in Figure 12). To transform this point force into the distributed moment formulated previously, the deflection caused on the tip (x=L) by this force must be equalled to the one caused by the moment at the same point (eq. (22)).

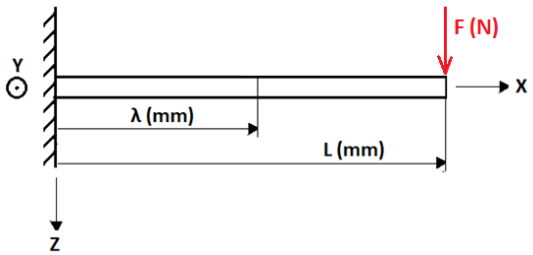

Figure 12: Tip force scheme

As shown in Figure 10 and Figure 11 at the point x=λ there is a change in the materials and area. The same principle applied for the continuity at this λ point must be applied here.

Torque equation of x within the range $0 \leq x \leq \mathrm{L}$:

$$M = -F(L - \mathrm{x}) \quad (24)$$

For $0 \leq x \leq \lambda$:

Inserting eq. (24) into (3) and integrating it two times over "x":

$$F(L - \mathrm{x}) = \sum(\mathrm{EI})^L w''$$

$$F\left(Lx - \frac{x^2}{2}\right) + C_1^L = \sum(\mathrm{EI})^L \mathrm{w}' \quad (25)$$

$$F\left(L\frac{x^2}{2} - \frac{x^3}{6}\right) + C_1^L \mathrm{x} + C_2^L = \sum(\mathrm{EI})^L w \quad (26)$$

Due to the characteristics of the structure, at x=0 both deflection and angle become null at this position and the constants $\mathrm{C}_1^{\mathrm{L}}$ and $\mathrm{C}_2^{\mathrm{L}}$ become null:

$$C_1^L = C_2^L = 0$$

Equations defining the behaviour for range $0 \leq x \leq \lambda$:

- $w(x) = \frac{F(3L-\mathrm{x})}{6\sum(\mathrm{EI})^L} x^2$ (27)
- $w'(x) = \frac{F(2L-\mathrm{x})}{2\sum(\mathrm{EI})^L} x$ (28)

For $\boldsymbol{\lambda \leq x \leq L}$:

As the torque equation (24), the equations for this part are the same as eqs. (25) and (26), but the constants are $\mathrm{C}_1^{\mathrm{R}}$ and $\mathrm{C}_2^{\mathrm{R}}$.

As explained before, the continuity at x= λ should be applied differentiating immediately right $(\sum(\mathrm{EI})^{\mathrm{R}})$ and left $(\sum(\mathrm{EI})^{\mathrm{L}})$ sides of this point.

By equalling $\mathrm{w}'(-\lambda) = \mathrm{w}'(+\lambda)$ in eqs. (25) and (28), but in eq. (25) using $\sum(\mathrm{EI})^R$ instead of $\sum(\mathrm{EI})^L$:

$$F\left(L\lambda - \frac{\lambda^2}{2}\right) + C_1^R = F(2L-\lambda)\frac{\sum(\mathrm{EI})^R}{2\sum(\mathrm{EI})^L}\lambda \quad \rightarrow$$

$$\rightarrow \quad C_1^R = F\left(L\lambda - \frac{\lambda^2}{2}\right)\frac{\sum(\mathrm{EI})^R}{\sum(\mathrm{EI})^L} - F\left(L\lambda - \frac{\lambda^2}{2}\right) \rightarrow$$

$$\rightarrow \quad C_1^R = F\left(L\lambda - \frac{\lambda^2}{2}\right)\left(\frac{\sum(\mathrm{EI})^R}{\sum(\mathrm{EI})^L} - 1\right) \quad (29)$$

Equalling $w(-\lambda) = w(+\lambda)$ in eqs. (26) and (27), but in eq. (26) using $\sum(\mathrm{EI})^R$ instead of $\sum(\mathrm{EI})^L$:

$$\left(L\frac{\lambda^2}{2} - \frac{\lambda^3}{6}\right) + C_1^R\lambda + C_2^R = \frac{\sum(\mathrm{EI})^R}{\sum(\mathrm{EI})^L}\frac{F(3L\lambda^2 - \lambda^3)}{6} \rightarrow$$

$$\rightarrow \quad C_2^R = \frac{\sum(\mathrm{EI})^R}{\sum(\mathrm{EI})^L}F(L\frac{\lambda^2}{2} - \frac{\lambda^3}{6}) - F\left(L\frac{\lambda^2}{2} - \frac{\lambda^3}{6}\right) - C_1^R\lambda \rightarrow$$

$$\rightarrow \quad C_2^R = F\left(L\frac{\lambda^2}{2} - \frac{\lambda^3}{6}\right)\left(\frac{\sum(\mathrm{EI})^R}{\sum(\mathrm{EI})^L} - 1\right) - C_1^R\lambda \rightarrow$$

Inserting eq. (29):

$$\rightarrow \quad C_2^R = F\left(L\frac{\lambda^2}{2} - \frac{\lambda^3}{6}\right)\left(\frac{\sum(\mathrm{EI})^R}{\sum(\mathrm{EI})^L} - 1\right) - F\left(L\lambda^2 - \frac{\lambda^3}{2}\right)\left(\frac{\sum(\mathrm{EI})^R}{\sum(\mathrm{EI})^L} - 1\right) \rightarrow$$

$$\rightarrow \quad C_2^R = F\left(\frac{\sum(\mathrm{EI})^R}{\sum(\mathrm{EI})^L} - 1\right)\left(-L\frac{\lambda^2}{2} + \frac{\lambda^3}{3}\right) \quad (30)$$

The equation for the displacement of the tip (x=L) for a load point, which is the load that is measured by the "Series 300B dual mode servo system" will be:

$$w(L) = \frac{F}{\sum(\mathrm{EI})^R}\left(\frac{L^3}{2} - \frac{L^3}{6} + \left(L^2\lambda - L\frac{\lambda^2}{2}\right)\left(\frac{\sum(\mathrm{EI})^R}{\sum(\mathrm{EI})^L} - 1\right) + \left(\frac{\sum(\mathrm{EI})^R}{\sum(\mathrm{EI})^L} - 1\right)\left(-L\frac{\lambda^2}{2} + \frac{\lambda^3}{3}\right)\right) \rightarrow$$

$$\rightarrow \quad w(L) = \frac{F}{\sum(\mathrm{EI})^R}\left(\frac{L^3}{3} + \left(L^2\lambda - L\lambda^2 + \frac{\lambda^3}{3}\right)\left(\frac{\sum(\mathrm{EI})^R}{\sum(\mathrm{EI})^L} - 1\right)\right) \quad (31)$$

Equalling eqs. (31) and (22) at x=L:

$$m = F\frac{\frac{L^3}{3} + \left(L^2\lambda - L\lambda^2 + \frac{\lambda^3}{3}\right)\left(\frac{\sum(\mathrm{EI})^R}{\sum(\mathrm{EI})^L} - 1\right)}{\frac{L^3}{3} + \mathrm{L}^2\lambda\left(\frac{\sum(\mathrm{EI})^R}{\sum(\mathrm{EI})^L} - 1\right) - \mathrm{L}\lambda^2\left(\frac{3}{2}\frac{\sum(\mathrm{EI})^R}{\sum(\mathrm{EI})^L} - 1\right) + \lambda^3\left(\frac{1}{2}\frac{\sum(\mathrm{EI})^R}{\sum(\mathrm{EI})^L} - \frac{1}{3}\right)} \quad (32)$$

By obtaining the force of the tip and inserting it into eq. (32), the moment that is generated by the PPy due to the swelling over a potential is obtained.

4.4. Gravity effect

The gravity can affect to the total deflection of the sample. It can greatly reduce the curvature and reduce the efficiency of the PPy actuator because a fraction of the energy is destined to counteract the weight force.

This effect should be tested to know if it has enough influence on the final curvature. The sample position is vertical as shown in Figure 13. In this position, when the PPy coating is greater and deflects more, the gravity has a greater effect than if it is in horizontal position, when the PPy coating is in right or left side, and the gravity is downwards.

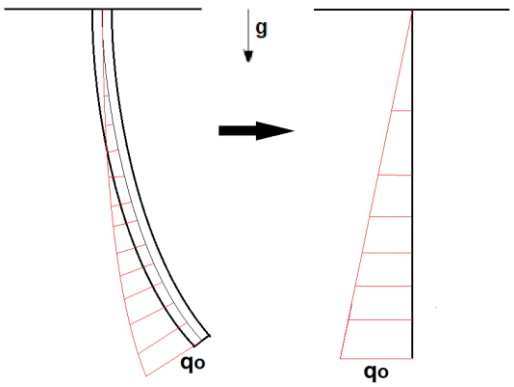

Figure 13: Gravity force approximation

To know how the gravity can affects the actuation efficiency, an important parameter to consider is the angle of curvature (θ) which has its higher value at the tip. A triangular distributed load can be considered as seen in Figure 13 because the higher is the angle, the higher the force perpendicular to the sample component is. This approximation is enough accurate to know it this effect should be considered.

The following Figure 14 shows the parameters to consider when analysing.

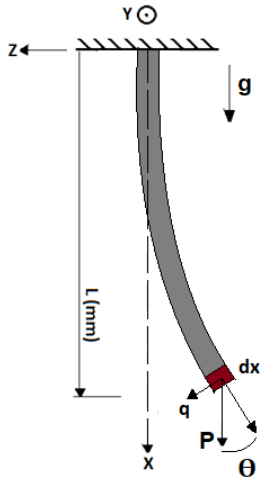

Figure 14: Gravity force scheme

As seen, the higher value of the force is at the tip. To obtain it, a small "piece" dx has been considered and the perpendicular component "q" of the force is:

$$q = \frac{mg}{L} dx \cdot \theta \quad (33)$$

To obtain the triangular distributed force:

$$qo = \frac{q}{2L} \cdot n \quad (34)$$

Where "n" is the number of dx divisions made.

From handbooks of mechanics (21), it is known that this distribution of force follows:

$$w_g(x) = \frac{q_o L^4}{120EI}\left(\frac{x^5}{L^5} - 10\frac{x^3}{L^3} + 20\frac{x^2}{L^2}\right) \quad (35)$$

For the position x=L:

$$w_g(L) = \frac{11 q_o L^4}{120EI} \quad (36)$$

5. Experimental and Theoretical Results & Discussion

5.1. ZIPwire™ Hydrophilic Experience

5.1.1. Stiffness ∑(EI)

For the ∑(EI) , as the ZIPwire has a tapered shape (Figure 15), a mean value of the second moment of area should be obtained to simplify the model.

Figure 15: ZIPwire

Measured Dimensions of the Nitinol core and Mechanical Properties for both, core and jacket (22), (23):

Tapered Length (mm)	dinitial (mm)	dtip (mm)	E core (MPa)	E jacket (MPa)
115	$0{,}410 \pm 0{,}001$	$0{,}187 \pm 0{,}001$	28000	500

Table 3: ZIPwire measured dimensions

For the ZIPwire, an iterative process in MATLAB make easier to obtain the second moment of area "I" mean value.

$$I_{metal} = 5\text{E} - 04 \text{ mm}^4$$

$$I_{coating}^{L} = \frac{1}{4}\pi r^4 - I_{metal} \quad (37)$$

Where "r" is the radius value of the coating.

With this approximation is obtained a simpler model for the "EI" product with a constant metal core and coating jacket:

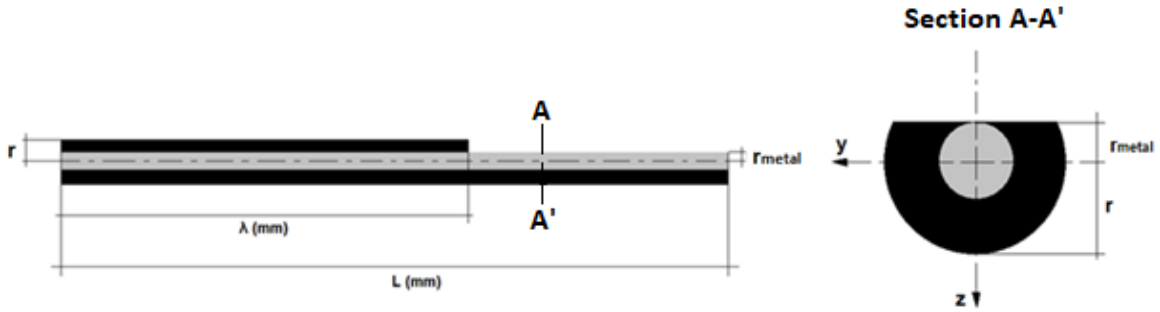

Figure 16: Wire approximation and cross-section area

The value of the "I" where part of the coating jacket has been removed for the attachment of the PPy is obtained by:

$$I^R_{coating} = \frac{1}{8}\pi r^4 + \int_{-r_{metal}}^{0} z^2 \cdot 2\sqrt{r^2 - z^2}\, dz - I_{metal} \quad \rightarrow$$

$$\rightarrow \quad I^R_{coating} = \frac{1}{8}\pi r^4 + \left|\frac{1}{4}\left(z\sqrt{r^2 - z^2}(2z^2 - r^2) + r^4 \tan^{-1}\left(\frac{z}{\sqrt{r^2 - z^2}}\right)\right)\right|_{-r_{metal}}^{0} - I_{metal} \quad (38)$$

If the following values are used:

$\mathrm{r} = 0.889/2$ mm

$\mathrm{I_{metal}} = 5\mathrm{e} - 04$

$\mathrm{r_{metal}} = \sqrt[4]{\frac{4 \cdot \mathrm{I_{metal}}}{\pi}}$ mm

From eqs. (37) and (38) it is obtained:

$I^L_{coating} = 0.0421 \;\; mm^4$

$I^R_{coating} = \; 0.0220 \;\; mm^4$

The factor for the second moment of area at the right part (where is attached the PPy) is shown:

$$I^R_{coating} = 0{,}52 \cdot I^L_{coating}$$

The final values for $\sum(EI)$:

$\sum(EI)^L = E_{metal} \cdot I_{metal} + E_{coating} \cdot I^L_{coating}$

$\sum(EI)^R = E_{metal} \cdot I_{metal} + E_{coating} \cdot 0{,}52 \cdot I^L_{coating}$

5.1.2. Measurements and Calculus Comparison

The size of the PPy affects to the force that it produces due to the current. For a larger polymer, the ions that can come into the structure is greater since it has more “storage space”.

To measure the force, two tests are going to be made. The first one consists on variate the thickness and the second one on variate the length of the PPy. This fact is important since if the force can be measured, the control of the catheter can be more precise and reliable.

The assumptions that are being taken in the theoretical results are the neglection of the gravity effect and the variation of stiffness of the PPy due to the low effect on the final deflection that they have. The thickness of the PPy is small enough to neglect it. This will be shown later.

In each wire, the experimental results and the theoretical are compared to see how the model fits the reality.

The equations that will be used to compare are eqs. (16), (17), (22) and (23), and the data has been stated previously.

5.1.2.1 Experimental Deflection Measurement

The typical deflection result is shown in Figure 17. The PPy is attached at the right part of the samples meaning that during reduction it bends to the left because ions get into the solid polymer (right picture to left picture) and during oxidation to the right because ions leave the solid polymer (left picture to right picture). This has been previously explained and can be seen in eq. (a).

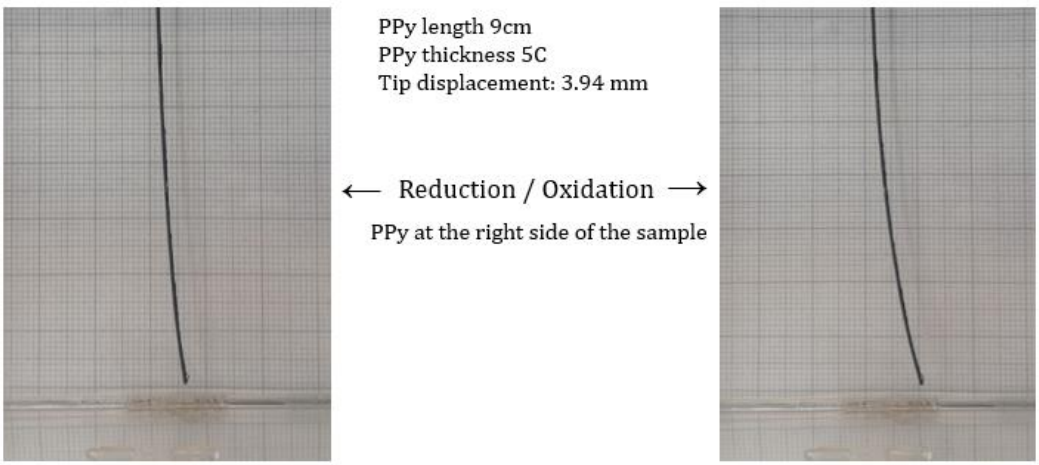

Figure 17: Bending of the sample

5.1.2.2 Constant Length, Different Thicknesses

The thickness increasement of PPy implies more ions and more expansion. The thicknesses studied are 2.5C, 5C and 7.5C all with a PPy length of 9cm. The potential difference applied is $\pm$0.7V.

In order to get the desired deflection some previous cycles must been applied to accommodate the PPy. For this purpose, the previously stated potentials have been applied each one 5 times respectively.

For the three thicknesses, the distance from the tip to the fixed part is 115 mm.

- 2.5C thickness:

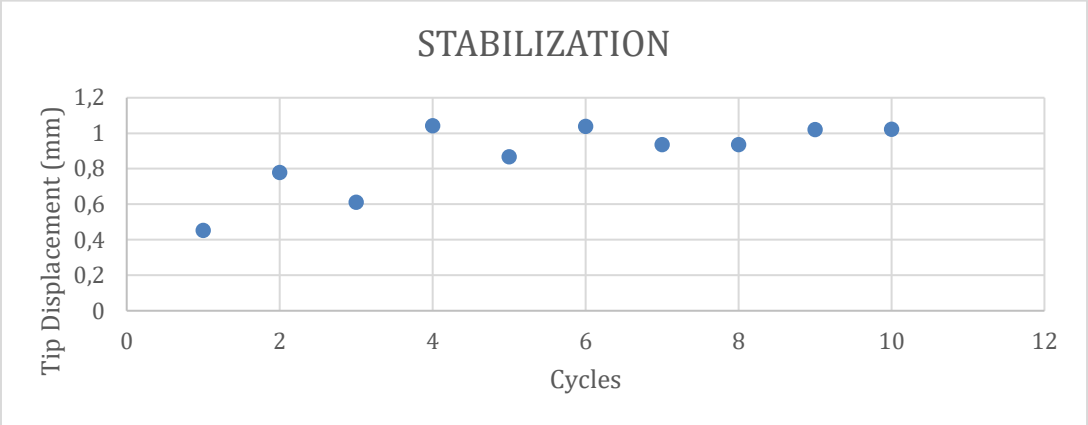

Figure 18: Stabilization

Here, in Figure 18, it can be seen that for 10 cycles, the PPy reaches a constant deflection since the 4th cycle. The following stabilization are similar or equal, so the following stabilizations will not be introduced.

Measured Tip Force = 5,34E-05 N

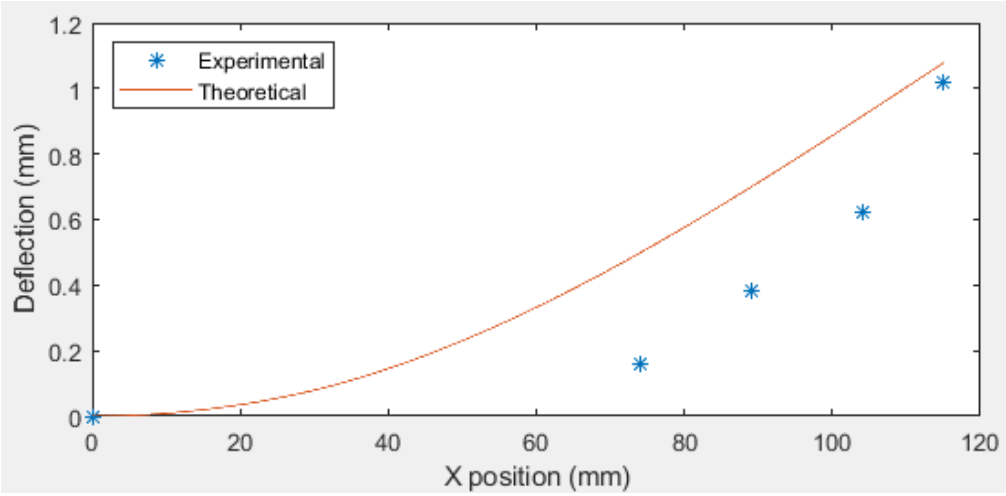

Figure 19: 2.5C length 9 cm comparison

In Figure 19, the final values of the deflections are similar enough, but the displacement along the wire is not due to that a constant core radius instead a tapered core shape has been considered.

- 5C thickness:

Measured Tip Force = 0,000206947 N

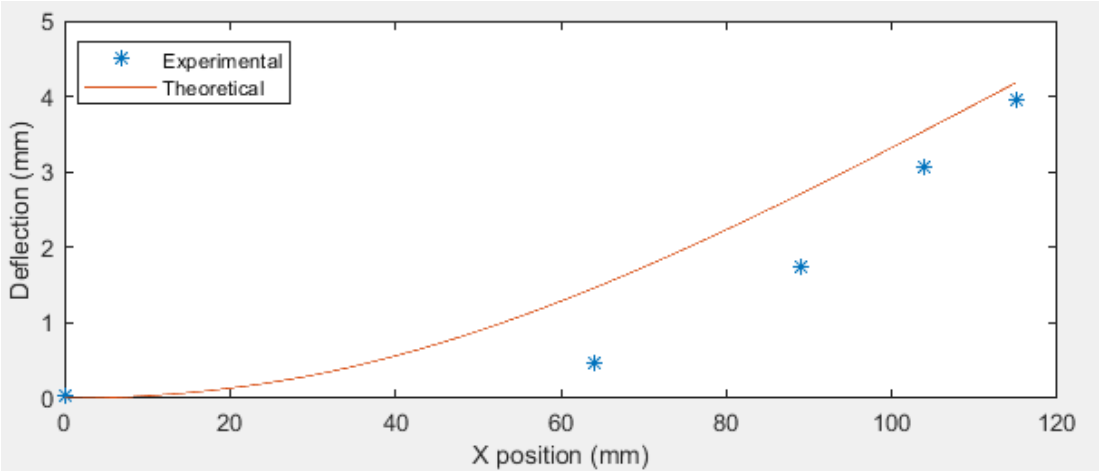

Figure 20: 5C length 9cm comparison

As in the 2,5C catheter, in Figure 20 it can be seen that the tip displacement of the theoretical model fits good enough with the experience, but the tendency does not.

- 7.5C thickness:

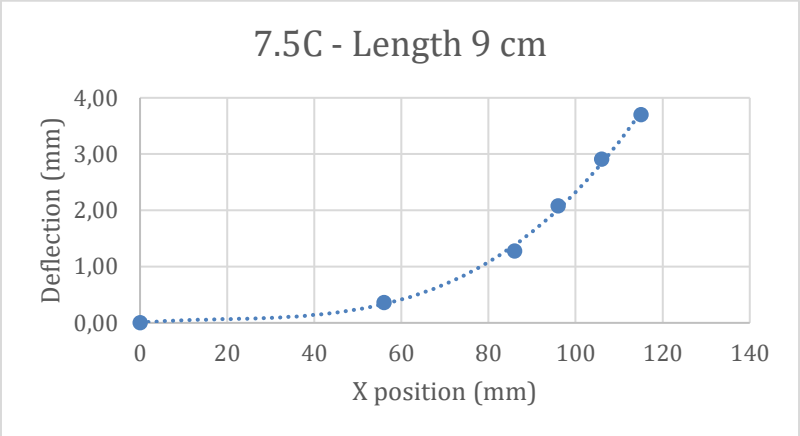

Figure 21: Experimental 7.5C Length 9cm Deflection vs position

About the 7.5C thickness catheter, in Figure 21, due to problems with the first measuring, the sample was re-polymerized. This fact affects to the attachment of the PPy to the metallic core and it does not produce the force that it should. It can be seen in the displacement in the Figure 21 since the displacement should be greater than the produces with thickness of 5C (3.96 mm) and we only obtain 3.70 mm.

The theoretical values have not been made since the force calculated was incorrect and the real charge was not saved.

5.1.2.3 Constant Thickness, Different Lengths

The length of PPy affects to the deflection of the tip since the force produced due to the shrinking and swelling is dependent on its size.

Theoretically, if the length of PPy is increased the number of ions that can get into the structure for the same potential is increased. In practice, the PPy coating lengths used will be of 2, 4 and 6 cm and a common thickness of 7.5 C. Not too large longitudes but enough to understand and corroborate the behaviour of this polymer. Now, the potential applied will be $\pm 0.4V$. This change in potential is in order to repeat the measurements if any problem of measuring appears, because for the previous values of potential, the measurements could not be repeated because the PPy has a limited cycle life and it could be reached with high potentials.

For the three lengths, the distance from the tip to the fixed part is 110 mm.

- 2 cm Length:

Measured Tip Force = 3,26546E-05 N

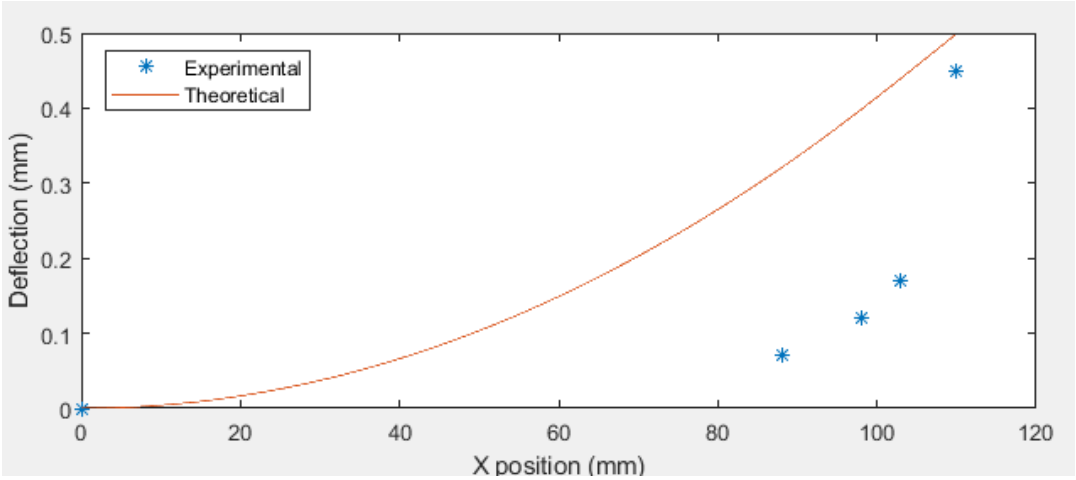

Figure 22: 7.5C length 2cm comparison

- 4 cm Length:

Measured Tip Force = 3,9745E-05 N

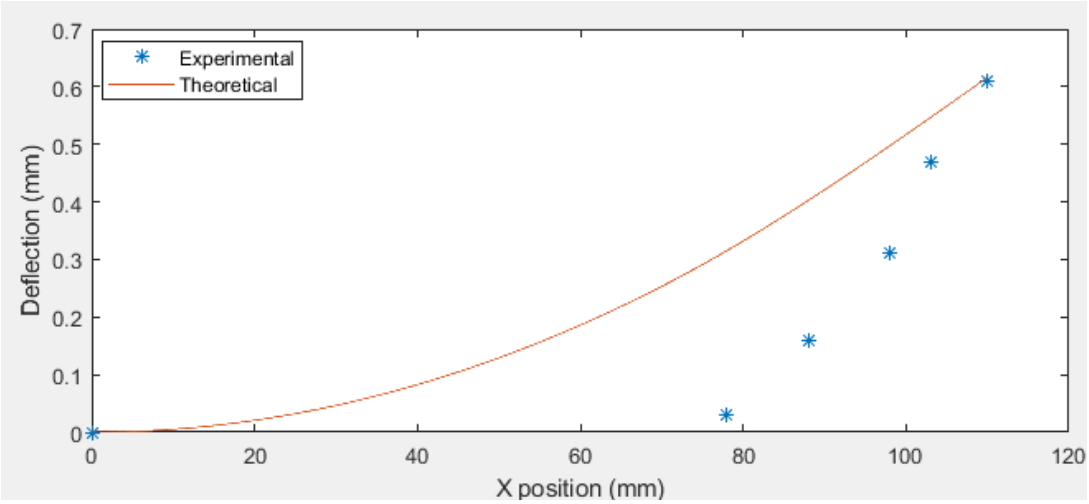

Figure 23: 7.5C length 4cm comparison

- 6 cm Length:

Measured Tip Force = 4.903E-05 N

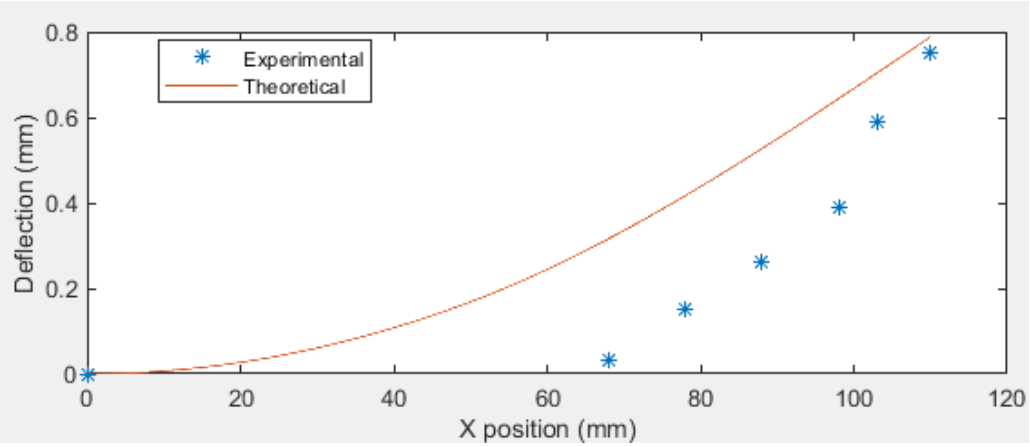

Figure 24: 7.5C length 6cm comparison

In all the graphs, Figure 22, Figure 23 and Figure 24, it can be seen that the model fits to the behaviour of the catheter. Due to the difficult modelling of a tapered shape as stated, a mean value of the stiffness has been considered, and this is the reason why the tendency line of the experimental and the theoretical results are not the same. For the theoretical one there is a more constant evolution than for the experimental one.

5.1.2.4 Final Results:

For the obtention of the PPY thickness, the micrometre has been used, and the following Figure 25 has been elaborated where it is shown how this value with respect to the charge applied to the creation of the polymer is. The samples measured have been the 7.5 C and an extra catheter of 13 C. With these thicknesses a linear interpolation has been made to get the desired thicknesses (2.5 C and 5 C).

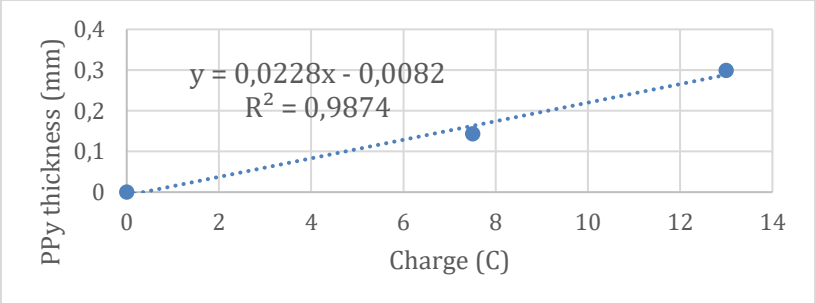

Figure 25: PPy thickness vs charge

The next tables, (Table 4 and Table 5), show the forces that actuates on each sample and the volumetric force that the PPy does for 2 different potentials. For the distributed torque “m” it is used the eq. (32). The distributed force “f” is calculated dividing the “m” over the PPy thickness and core radius. And calculating the cross-section area of the PPy and dividing the “f” over this area the volumetric force is obtained.

PPy dimensions	PPy thickness (mm)	Vertical Tip Force (N)	Distributed Torque "m" (N)	Distributed Force "f" (N/mm)
2.5C Length 9cm	0,0487	5,34E-05	5,65667E-05	3,09E-04
5C Length 9cm	0,1057	0,000207	2.19395E-04	10,37E-04
7.5C Length 2cm	0,1627	3,27E-05	1.20419E-04	5,01E-04
7.5C Length 4cm	0,1627	3,97E-05	7.51438E-05	3,13E-04
7.5C Length 6cm	0,1627	4,90E-05	6,53332E-05	2,72E-04

Table 4: Obtained forces transformation 1

Potential Difference (V)	PPy dimensions	Distributed Force "f" (N/mm)	Cross section Area (mm2)	Volumetric Force (N/mm3)	Mean Force (N/mm3)
±0,7	2.5C Length 9cm	3,09E-04	8,90E-03	3,47E-02	3,39E-02
	5C Length 9cm	10,37E-04	3,13E-02	3,31E-02	
±0,4	7.5C Length 2cm	5,01E-04	6,46E-02	7,76E-03	5,61E-03
	7.5C Length 4cm	3,13E-04	6,46E-02	4,85E-03	
	7.5C Length 6cm	2,72E-04	6,46E-02	4,21E-03	

Table 5: Obtained forces transformation 2

The volumetric force for all the samples with the same potential should be equal. As it is not since the PPy surface is irregular and the micrometre measures the thicker part of the PPy, it is necessary to obtain the mean value of the volumetric forces with a same potential.

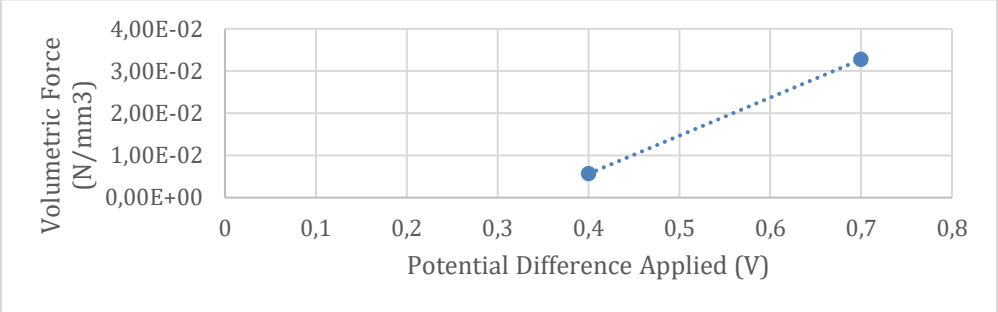

Figure 26: Volumetric force vs potential

The evolution of force respect to potential from Figure 26 follows a linear evolution which correlates with the theory of the force due to shrinkage and swelling. With this linear evolution, for a zero volumetric force, the potential would be around 0.35 V. The polymer needs a minimum potential difference in order to start the swelling or shrinkage.

This evolution is not realistic because there are only two points, but it gives an overview to know if the forces obtained are accurate enough to the theory of the force that generates the PPy with respect to the potential applied.

PPy dimensions	Experimental Tip Displacement (mm)	Theoretical Tip Displacement (mm)	Theoretical Tip Angle (degrees)
2.5C Length 9cm	1.02	1.0779	0.8524
5C Length 9cm	3.96	4.1808	3.3034
7.5C Length 2cm	0.45	0.4992	0.4902

7.5C Length 4cm	0.61	0.6160	0.5722
7.5C Length 6cm	0.75	0.7883	0.6947

Table 6: Experimental and theoretical final tip deflections and angles comparison

About the tip displacement, the values are almost exact, which means that the model is accurate with the reality behaviour.

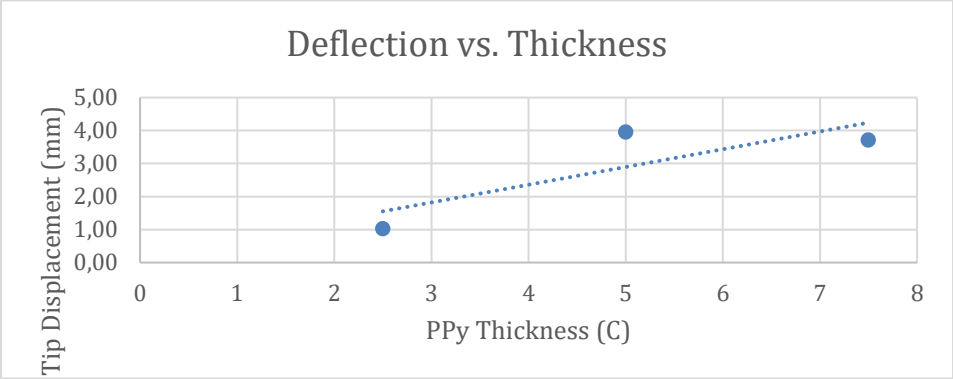

Figure 27: Experimental Deflection vs Thickness considering 7.5 C

As stated before, the 7.5C thickness does not move as it should (Figure 27). The following figure without considering the 7.5C shows the real tendency.

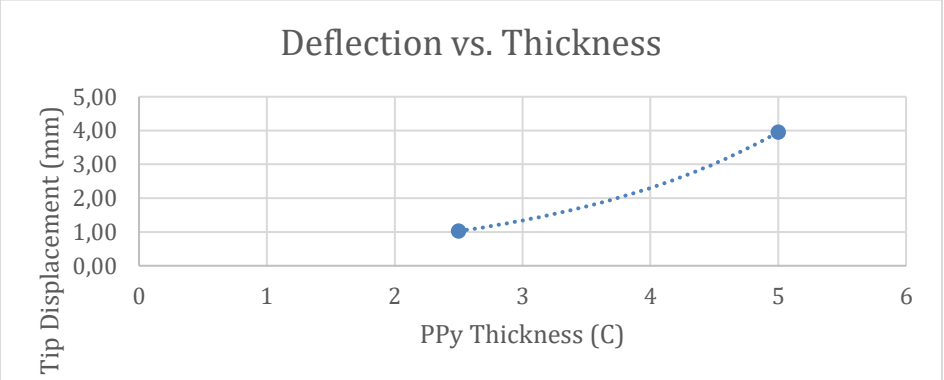

Figure 28: Experimental Deflection vs Thickness

In Figure 2828, the increasement of the thickness with constant length has 2 consequences. The first one is that as the volume is increasing, the force produces will be greater. The second one is that as the thickness is increased, the distance at which the force is applied is greater. With these 2 consequences, a greater moment is achieved. Therefore, the behaviour follows an exponential deflection evolution vs the PPy thickness instead of a linear tendency.

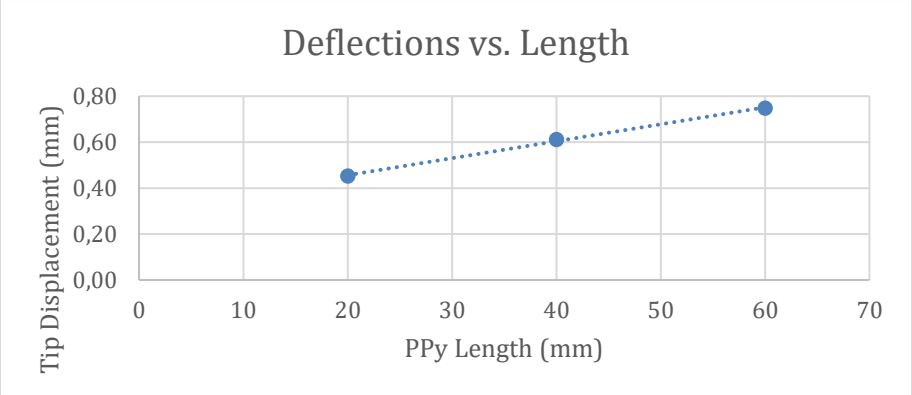

Figure 29: Experimental Deflection vs PPy length

In the Figure 29, the evolution of the tip displacement changing the PPy length with a constant thickness, follows a linear tendency. However, this line does not tend to 0, as expected. This is because the tapered shape, and the PPy which is attached to the thinner part of the core (tip), has a larger effect on the deflection.

5.1.3. Polypyrrole "EI" Effect

When the theoretical model is implemented in Matlab, the thickness of the PPy has been neglected due to the small differences in the deflections with and without PPy. This small difference is because the thickness that have been used does not affect the total stiffness. If it would be thicker, it could not be neglected.

To corroborate this, the PPy thickness has been implemented in the sample with the biggest tip displacement (5C). Also, the variation of Young's Modulus due to oxidation and reduction is shown, and there is no a big variation (24).

Using the eq. (22) these are the results:

	Tip displacement (mm)
Without consider PPy	4.1808
Considering PPy (E=820 MPa)	4.1091
Considering PPy (E=900 MPa)	4.1023

Table 7: PPy stiffness effect

5.1.4. Numerical Gravity Effect

About the gravity effect, the tip displacement using eq. (36) is shown in the next table:

PPy dimensions	Tip deflection due to Gravity (mm)	Theoretical Tip deflection (mm)	Gravity Influence (%)
length = 9cm 2.5 C	0.0676	1.0779	6.27
length = 9cm 5 C	0.2619	4.1808	6.26
length = 2cm 7.5 C	0.0326	0.4992	6.52
length = 4cm 7.5 C	0.0380	0.6160	6.17
length = 6cm 7.5 C	0.0461	0.7883	5.85

Table 8: Gravity influence

The gravity effect is between 5 – 7 %. This percentage can be neglected because it does not have a considerable effect in the final position.

5.2. Amplatz Super Stiff™ Experience

5.2.1. Stiffness ∑(EI)

For the ∑(EI) , as the Amplatz has a coil tip (Figure 1), a mean value of the second moment of area should be obtained to simplify the model.

Due to the difficulty of calculating by hand the second moment of area of a coil beam (Amplatz Guidewire), the most accurate and simplest way of obtaining it is the use of ANSYS to get the total stiffness $\sum(EI)^R$. This $\sum(EI)^R$ is used to implement in the deflection and curvature eqs. (22) and (23) for the right part. About the left part it has been considered that it is a beam with a circular cross-section area.

To model the coil, it has been used a micrometre to measure the dimensions. Each measurement has been made 3 times. The dimensions are in the Table 9.

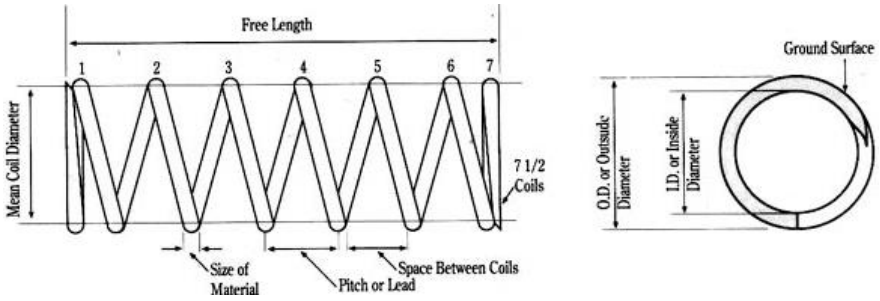

Figure 30: Coil structure

Coil Length (mm)	60
Inner Diameter (mm)	0.701 ± 0.001
Outer Diameter (mm)	0.965 ± 0.001
Pitch (mm)	0.436 ± 0.001
Size of Material (mm)	0.289 ± 0.001
Space Between Coils (mm)	0.147 ± 0.001

Table 9: Amplatz coil measurements

Moreover, as seen in Figure 1, the coil has an internal wire. It is composed by a short-tapered part of 3 cm, and a straight constant part of 6 cm. The diameter of the constant part is 0.141 ± 0.001 mm. The tapered part has not been implemented since the diameter has a great increase, so the stiffness is greater, and the movement of this part is null.

Modelling it and applying a known force a deflection is obtained in Figure 311.

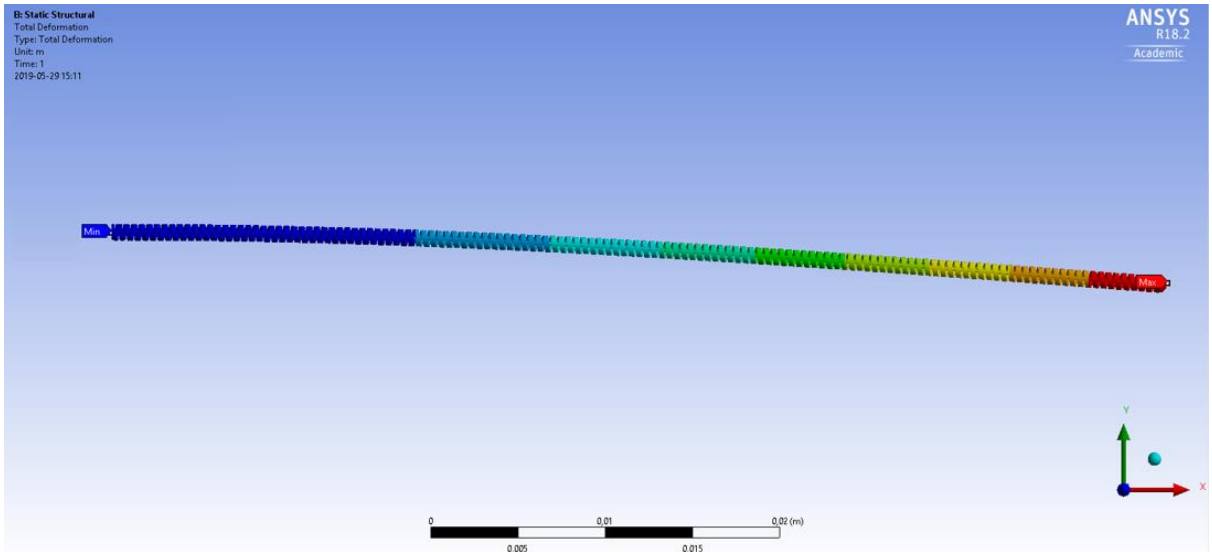

Figure 31: Amplatz coil tip ANSYS

The force has been applied at the tip and the results obtained are shown in the following table:

Force (N)	Tip Displacement (mm)
0.000100	0,9649
0.000192	1,8526

Table 10: Ansys Amplatz tip displacement

From beam theory equations in handbooks, it is known that for a point force at the tip, the deflection is:

$$w(L) = \frac{FL^3}{3\sum EI}$$

By using the table results and data the $\sum EI$ obtained with both forces is:

$$\sum EI = 7{,}462\ Nmm^2$$

5.2.2. Measurements and Calculus Comparison

The difficulties to polymerize the coil of the guidewire has made impossible to measure experimentally the deflection of the samples. These difficulties come since the sample is made by stainless steel 316 with a thin coating. The PPy is attached all around the guidewire making small deflections, causing shrinkage of the coil and difficult to see where the PPy is.

The only part which has a considerable deflection is the floppy part. Now, with the volumetric forces used in the ZIPwire, the values of the tip displacement in the Amplatz SuperStiff are calculated with eq. (22):

For $\pm$0.7 V, the volumetric force is 3,39E-02 N/mm3.

The length considered is going to be the coil length because the part without coil has a great stiffness respect to the one obtained in the coil and this makes the attachment of PPy in that part useless.

Fixed Length (mm)	Polymerized Length (mm)	R_{outer} (mm)	R_{inner} (mm)	R_{mean} (mm)
110	60	0,4826	0,3506	0,4166

Table 11: Amplatz coil measurements

We are going to consider that the area of the PPy is a quarter of a total circle area and the force "f" is applied at a distance R_{mean}, as it can be seen in Figure 32.

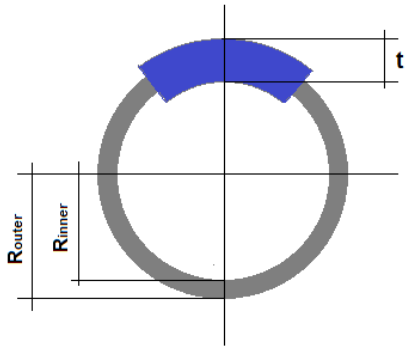

Figure 32: PPy attachment scheme

The volumetric force can be obtained from Table 5 for a potential of ± 0.7 V, and by using eq. (22):

PPy dimensions	Area (mm2)	Volumetric Force (N/mm3)	Distributed Force "f" (N/mm)	Tip Displacement (mm)
length=6cm 2.5C	0.0319	3.39E-02	1.06E-03	4.2767
length=6cm 5C	0.0692	3.39E-02	2.35E-03	9.4813

Table 12: Theoretical displacement for a known PPy thickness

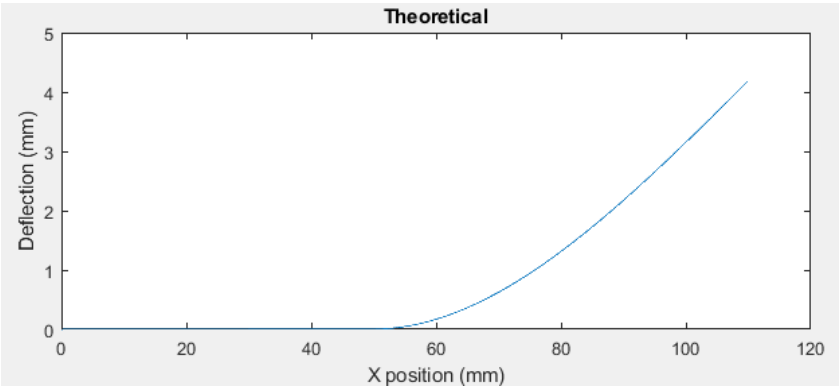

Figure 33: Amplatz: 2.5C Deflection

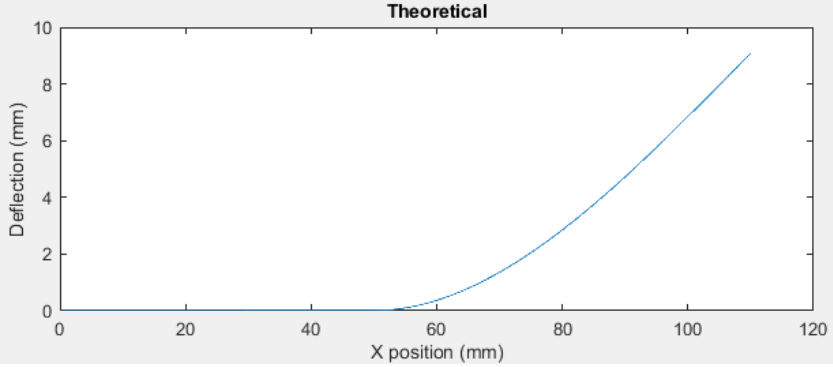

Figure 34: Amplatz: 5C Deflection

The deflection values obtained for the 2.5C and 5C shown in Table 12 should be compared with experimental results for these PPy dimensions, but as it stated before, due to problems with polymerization it could not be possible. Since the fixed length is 110 mm, this displacement shown in Figure 333 and Figure 34Figure 34 could be possible.

6. Conclusion and Future work

Through the developed theoretical model and comparing with the experimental results obtained in the laboratory, can be seen that the model seems to predict the bending of the ZIPwire and the Amplatz Super Stiff wire.

Moreover, the dimensions of the PPy due to the force that they produce have a big influence on the final deflections. This force has a great dependence on the potential applied as seen. Another fact to consider is that variating the PPy length with constant thickness and variating the thickness with constant PPy length, it can achieve different deflections, and different curve tendencies. The first curve tendency has a linear evolution; and the second one follows an exponential evolution. This different behaviour could be interesting for different purposes such as the deflection which wants to be obtained and the amount of PPy wanted to use.

To corroborate the correct functioning of this theoretical model, it should be tested by comparing it with another experimental results. An important fact to consider is that for the Amplatz SuperStiff guidewire, it has been only used theoretical results due to the difficulties of polymerization these kinds of structures and its complex shapes.

The creation of PPy based active guidewires is a great step for the medical field evolution. The development of a model that controls the bending of this guidewires would be a great progress in order to know the amount of conducting polymer needed to achieve the desired deflection.

References

1. *Minimally Invasive and Robotic Surgery.* **Michael J. Mack, MD.** February 7, 2001.

2. *Applications of conducting polymers and their issues in biomedical engineering.* **Rajeswari Ravichandran, Subramanian Sundarrajan, Jayarama Reddy Venugopal, Shayanti Mukherjee and Seeram Ramakrishna.** 2010.

3. *Conducting Polymer Based Active Catheter for Minimally Invasive Interventions inside Arteries.* **Tina Shoa, John D. Madden, Niloofar Fekri, NigelR. Munce, Victor XD. Yang.**

4. **Laura Valero Conzuelo, Joaquín Arias-Pardilla, Juan V. Cauich-Rodríguez, Mascha Afra Smit and Toribio Fernández Otero.** *Sensing and Tactile Artificial Muscles from Reactive Materials.* 2010.

5. **Jager, Edwin.** *Conducting Polymer Actuators for Medical Devices and Cell Mechanotransductio.* 2013.

6. **Lashidani, Tina Shoa Hassani.** *ENGINEERING ASPECTS OF POLYPYRROLE.* 2010.

7. **Polypyrrole Wikipedia. [En línea] 2019. https://en.wikipedia.org/wiki/Polypyrrole.**

8. **Shanbhag, Rakshith.** ***POLYPYRROLE ACTUATED URETERAL GUIDEWIRE.*** **2016.**

9. **Electrolyte Wikipedia. [En línea] 2019. https://en.wikipedia.org/wiki/Electrolyte.**

10. **Anand Shah BSab Charles Lau MDaS. William Stavropoulos MDa Alexander Nemeth MDa Michael C.Soulen MDa Jeffrey A.Solomon MD, MB AaJeffrey I.Mondschein MDa Aalpen A.Patel MDa Richard D.Shlansky-Goldberg MDaMaximItkinMDaJesse L.ChittamsMScScott O.TrerotolaMDa.** ***Comparison of Physician-rated Performance Characteristics of Hydrophilic-coated Guide Wires.***

11. **C. Michael Gibson, M.S., M.D. WikiDoc Guidewire. [En línea] 28 de January de 2013. https://www.wikidoc.org/index.php/Guidewire.**

12. **Crummy, Yoichi KikuchiVirgil B. GravesCharles M. StrotherJohn C. McDermottStephen G. BabelAndrew B.** ***A new guidewire with kink-resistant core and low-friction coating.*** **1989.**

13. **Ranaweera, Priyantha. WikiDoc. [En línea] 2013. www.wikidoc.org/index.php/Guidewire.**

14. **Scientific, Boston. ZIPWire Boston Scientific. [En línea] 2019. https://www.bostonscientific.com/en-US/products/guidewires/zipwire.html.**

15. **—. Amplatz SUperStiff Boston Scientific. [En línea] 2019. https://www.bostonscientific.com/en-US/products/guidewires/amplatz-super-stiff.html.**

16. **Leite, Márcio Nimer.** ***ESTUDIO DEL COMPORTAMIENTO AMBIENTAL DEL SULFONATO DE ALQUILBENCENO LINEAL.*** **2007.**

17. **PalmSens. PalmSens. [En línea] 2019. https://www.palmsens.com/product/emstat/.**

18. Honeychurch, K.C. *Printed thick-film biosensors.* s.l. : Printed Films, 2012.

19. Instruments, BioLogic Science. Reference electrodes & porous glass frits. [En línea] 2016. https://www.bio-logic.net/accessories/electrodes/reference-electrodes-porous-glass-frits/.

20. Systems, Bioanalytical. Bioanalytical Systems. [En línea] https://www.basinc.com/products/ec/ref.

21. Dahlberg, Tore. *Formulas in Solid Mechanics.* Linköping, Sweden : s.n., 2002.

22. Chemistry Learner. [En línea] 2019. https://www.chemistrylearner.com/nitinol.html.

23. PTFE wikipedia. [En línea] https://en.wikipedia.org/wiki/Young%27s_modulus.

24. Tina Shoa, Tissaphern Mirfakhrai and John D.W. Madden. *Electro-stiffening in polypyrrole films: Dependence of Young's Modulus on oxidation state, load and frequency.* s.l. : ELSEVIER, 2009.

25. Gursel Alici, Nam N. Huynh. *Predicting force Output of trilayer polymer actuators.* 2006.

26. Chen, Zhaojiang. Research Gate. [En línea] https://www.researchgate.net/figure/Temperature-dependence-of-a-Youngs-modulus-and-b-velocity-of-sound-of-nitinol-In_fig1_277574551.